Journal of Materials Science: Materials in Electronics (2019) 30:259–265
https://doi.org/10.1007/s10854-018-0288-2

Enhancing the Co gas sensing properties of ZnO thin films with the decoration of MWCNTs

F. Özütok[1] · Irmak Karaduman Er[2] · S. Acar[2] · S. Demiri[3]

Received: 12 April 2018 / Accepted: 24 October 2018 / Published online: 28 October 2018

Abstract
Multi-walled carbon nanotubes (MWCNTs) onto flower-like patterned ZnO seed layers were prepared by spin coating method. The etching of the MWCNTs was examined by HCl acid treatment. The effect of structural, morphological and elemental properties of the ZnO/MWCNTs were determined by XRD, SEM, and EDX, respectively. The gas sensing properties of ZnO seed layer and MWCNT/ZnO nanocomposites were studied as a function of operating temperature and gas concentration. The incorporation of MWCNT were given results such as reducing the operating temperature to 70 °C and enhancement in sensor response for 25 ppm CO gas. It was obtained that the highest sensing response of 62% at 70 °C for raw-MWCNTs/ZnO sensor as compared to etched-MWCNT/ZnO and ZnO sensor which gave a sensing response of 19% and 21% at operating temperature of 70 °C and 150 °C, respectively. Results showed that the deposition of metal oxide sensors with MWCNT is a promising strategy for improvement of CO gas sensing properties.

1 Introduction

Carbon monoxide exposure is still one of the leading causes of gas poisonings, and it causes many deaths annually in all over the world [1]. The affinity of hemoglobin for carbon monoxide compared to oxygen is 200–250 times higher [2]. Carbon monoxide forms carboxyhemoglobin (HbCO) in the blood when combining with hemoglobin. As a result of this, hemoglobin was unable effectively to transport oxygen to the tissues. Furthermore, it reduces its oxygen-carrying capacity of the blood, giving rise to hypoxia [3], which if not treated can lead to unconsciousness and even death.

In the literature, in order to overcome side effects of the CO, CO carbon films were used. Therefore, a high-performance CO sensor, that is one that combines high sensitivity and selectivity, fast response/recovery, low consumption and detection limit, good portability are very necessary and important for monitoring the living/working environment and healthy status of human beings [4]. Metal oxide semiconductor (MOS) gas sensors have been extensively researched due to their applicability in various fields. In this regard the highly stable ZnO is one of the most important MOS materials exhibiting a bap gap of 3.37 eV at room temperature and a high excitation bond energy of 60 meV [5]. Owning to its unique physicochemical properties, ZnO has been applied in a variety of areas such as piezoelectric, solar cells, optical devices, as well as gas sensors.

Carbon nanotubes (CNTs) still remain at forefront of nanoscale materials research in the past decade, while the interest in their properties is growing ever since their discovery. The exceptional and unique properties of CNTs offer a great advantage for the production of improved composites, while their applications as a matrix element depends primarily on the relationship between the matrix and the other material [6]. The introduction of defects such as atom vacancies, functional groups and stone wall defects on nanotubes can enhance the sensitivity towards different gases. These defect sites lower the activation energy barrier thus enabling chemisorptions of analytes on the surface of CNTs and make room temperature measurements possible. Multi-walled carbon nanotubes (MWCNTs) are nanoscale materials that comprise of several concentric single walled carbon nanotubes (SWCNTs) and exhibit diameters in the range of 5 and 30 nm. The MWCNTs exhibit excellent optical, mechanical and electrical properties and appear as suitable material for

✉ F. Özütok
fatmaozutok@comu.edu.tr

[1] Department of Physics, Science Faculty, ÇOMU, Çanakkale, Turkey

[2] Department of Physics, Science Faculty, Gazi University, Ankara, Turkey

[3] Faculty of Technological Sciences, Mother Teresa University, Skopje, Macedonia

nanocomposites. Nanocomposites employing MWCNTs and some other materials such as polymer, metal-alloys, metal-oxides, ceramic etc. have been previously reported, and some of these nanocomposites find applications in design of supercapacitors, gas sensors, smart window and photovoltaic cell devices [7, 8].

More recently, CNTs/metal oxide composites sensors based on MWCNTs have been reported to detect CO, NH and NO at room temperature and acceptable sensitivity was detected at higher temperatures. The electrical conductivity of these composites is depend on amount of surrounding gases. Therefore, these structures presents a great potential as a new gas sensing material for CO gas. There is insufficient literatüre for MWCNT/ZnO composites as sensors for CO gas. For the detection of CO, Alharbi et al. demonstrated that surface functionalization of MWCNTs by ZnO nanoparticles was increased sensing properties of MWCNTs as sensors at room temperature [9]. The improved gas sensing properties of ZnO/MWCNTs nanocomposites were characterized in terms of effective electron charge transfer between CO gas molecules and the interfaces between ZnO/MWCNTs as well as MWCNTs surface. Khanderi et al. reported that the nanostructured ZnO/MWCNT composite showed better sensing performance compared to MWCNT in the detection of low level CO gas [10]. Hojati et al. analyzed that MWCNT into the ZnO sensors enhanced the sensitivity, and showed considerable high sensitivity and fast response to CO at around 100 °C operating temperature, compared to undoped ZnO sensors [11]. The advantage of this sensor was in its small size, very thin structure and low working temperature, fast response and recovery time and low value of the dedection limit (ppm) of CO gas was obtained.

The researchers have manifested that MWCNTs introduction into ZnO could enhance its sensing properties by increasing the surface area and also the gas diffusion by formation of nanochannels in the ZnO [12]. ZnO is a very suitable host matrix counterpart for MWCNT in the production of nanocomposites, due to its high electron mobility, porous surfaces and abundance in the nature [13]. In addition, small amount of MWCNT can already fine-tune the resistance of the sensing layer, which expands its operational capabilities at low temperatures.

However, depending on the synthetic route, MWCNT/ZnO nanocomposites can also exhibit some limitations in terms of their long-term stability, presence of defects and reliability. The possibility to circumvent some of these limitations have also motivated further research on the MWCNT/ZnO nanocomposites [14]. A variety of MWCNT/ZnO synthesis methods have been reported in the literature and these includes atomic layer deposition (ALD) [15] microwave irradiation heating [16], electrochemical deposition [17] and spin coating [18]. Among the former, spin coating is frequently preferred because of its effective, facile and energy-efficient method. Spin coating methods have low process temperatures, higher homogeneity and purity of product materials. Molecular scale homogeneity can be obtained directly in the solution.

In this study, room temperature spin coating method is used to investigate the MWCNTs with and without etching onto flower-like patterned ZnO seed layers. The temperature dependent gas sensing studies showed two improvements; (i) a decreased operating temperature of the sensors from 150 to 70 °C (ii) an increased response of sensors the from 21 to 62% after decoration MWCNTs.

2 Materials and methods

2.1 Etching of MWCNTs

Raw MWCNTs were purchased from the Nanografi company at the Middle East Technical University (METU), Turkey. The purchased raw MWCNTs have average length of 1.5 micron and 10% metal impurities (Fe, Co, Cu and Zn elements were detected by EDX with differential ratios). HCl (12M) was purchased from Sigma-Aldrich, was used to induce etching. Raw MWCNTs were annealed at 400 °C for 9 h before they were refluxed in HCl acid bath. Then, acidic solution was filtered by double distilled water in order to remove MWCNT surface residues. Finally, MWCNTs were dried at 100 °C in the furnace. This procedure was repeated for several times.

2.2 Synthesis of nanocomposites

ZnO films, formed in a chemical bath deposition, were used as a seed layer which explained by our earlier study [19]. Raw and etched MWCNTs are mixed in ultrasonic bath, containing ethanol. Small amount both raw and etched MWCNTs containing ethanol solutions were dropped onto ZnO seed layer by spin coating. Ethylene glycol and triethylamine (TEA) were used as a solvent and stabilizer, respectively (1:1). The speed was adjusted to 800 rpm and this procedure repeated 2 times at room temperature. Finally, both of nanocomposites were annealed at 250 °C in the furnace. Pure ZnO, raw-MWCNTs/ZnO and etched-MWCNTs/ZnO were labelled as pure ZnO, rMWCNTs/ZnO and eMWCNTs/ZnO, respectively.

2.3 Characterization of nanocomposites

The crystal structures and orientations of nanocomposites were determined by Rigaku SmartLab X-ray diffractometer employing CuK_{α} (1.5406 Å) radiation with 0.0130 step size which was operated under 40 mA and 45 kV with powder method. The surface morphology of

nanocomposites was investigated by using JEOL JSM-7100F-SEM (Scanning Electron Microscope). Elemental microanalysis (wt%) of nanocomposites was determined by OXFORD Instruments X-Max EDX (energy-dispersive X-ray spectrometer) which had been attached to SEM.

The gas sensing performance of the thin films have been tested using a special computer-controlled measurement system has been fully detailed in our previous papers [20, 21]. This measurement system consists of Keithley 2400 Source-meter, modified sensor cell, Lake-Shore 325 temperature controller, MKS flow controllers (MFC), humidity sensor. The thin films have been evaluated by measuring the resistance change at various CO concentrations from 5 to 50 ppm. The air flow rate, under the same conditions, was kept constant in order to observe the behavior of different concentrations. In order to have a stable sensing, prior exposure to CO the sensor cell was exposed to dry air for 20 min. Mass flow controllers (MKS Series) have controlled the gas concentration in the test chamber. The data has been measured by Keithley 2400 SourceMeter collected in real-time using a computer. The relative humidity has been kept constant 25% and has been monitored by a Honeywell HIH-4000 humidity sensor.

3 Results and discussions

Based on the SEM images in Fig. 1, both nanocomposites exhibited reticular and randomly distributed MWCNTs and irregular flower shaped ZnO formations. Dimensions of nanopetal ZnO structures nearly were similar and ~ 200–300 nm. In eMWCNTs/ZnO nanocomposites, MWCNTs showed much more aglomerative formations with aggressive HCl acid etching thus non-homogeneous distribution was observed in Fig. 1b. Additionally, MWCNTs showed more cloistered on ZnO seed layers so MWCN/ZnO connectivity increased in eMWCNTs/ZnO samples. The agglomerative phases and ZnO nucleus centers damaging is likely to be caused by the formation of hydroxyl groups at the ends of MWCNTs during the etching process or due to the changes in the chemical environment during the seed ZnO layer formation (i.e. formation of surfactant-inorganic species) [22].

XRD patterns of rMWCNTs/ZnO and eMWCNTs/ZnO nanocomposite films are depicted Fig. 2a. It was also shown that impurity peaks which related to ambient compounds were not detected. In the 2θ range of 20°–30°, substrate effect was more dominant. All of the diffraction peaks could be represented as ZnO hexzagonal wurtzite crystal structure with space group of $P6_3mc$ (186) (JCPDS Card No: 36-1451). (100), (002), (101), (110), (103), (112) and (201) planes in

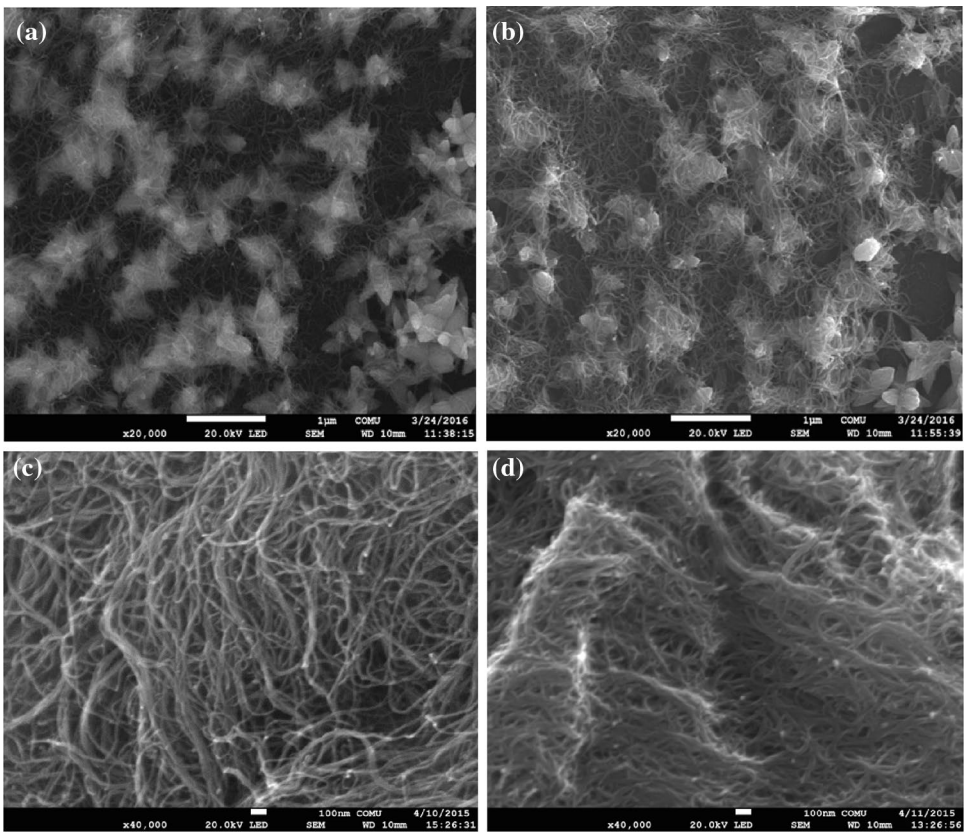

Fig. 1 SEM images of **a** rMWCNTs/ZnO and **b** eMWCNTs/ZnO nanocomposites **c** raw MWCNTs **d** HCl etched MWCNTs

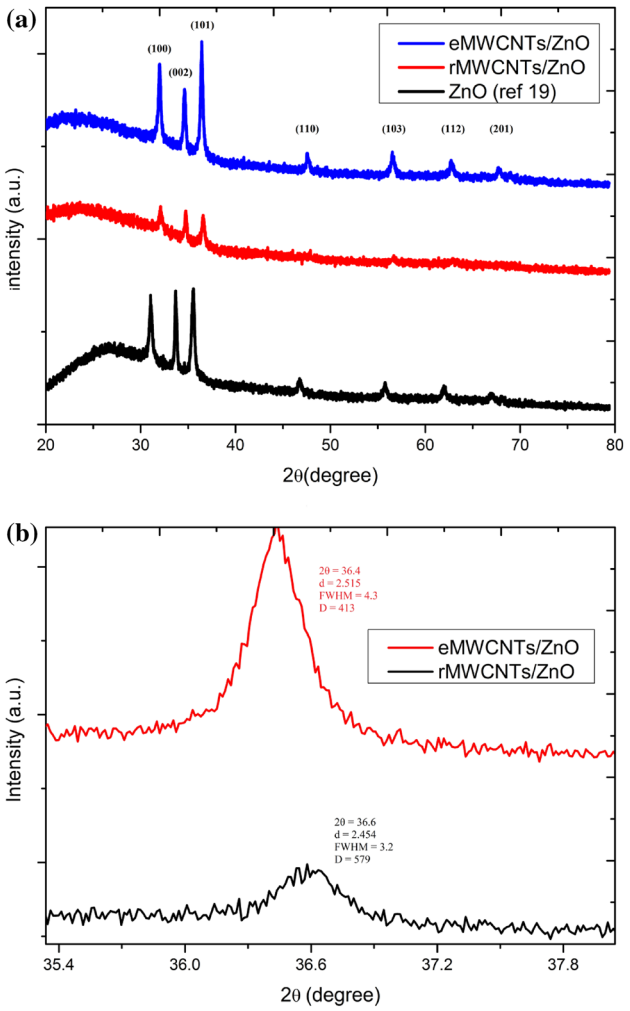

Fig. 2 X-ray diffraction patterns of rMWCNTs/ZnO and eMWCNTs/ZnO nanocomposites (**a**), 2θ, d, FWHM and D values for (101) preferential orientation (**b**)

2θ = 31.7°, 34.4°, 36.2°, 47.5°, 56.6°, 62.8° and 67.9° could be attributed to ZnO crystals. There was a disappearance of MWCNT characteristic peaks (JCPDS Card No:41-1487) probably due to the small amount of C content in the nanocomposites and the absence of MWCNTs aggregated pores [23]. Etching of MWCNTs was not cause an increase of defect sites in the range of 2θ = 30°–40° [24]. Compared to our synthesized ZnO seed layer-XRD profile with similar method, the crystallinity of ZnO in eMWCNTs/ZnO samples was improved by emerging MWCNT functional groups such as OH, COOH and COCl as clearly showed in Fig. 2a [25]. The crystallinity size was determined by Debye–Scherrer formula, given by Eq. 1;

$$D = \frac{k\lambda}{\beta \cos\theta} \quad (1)$$

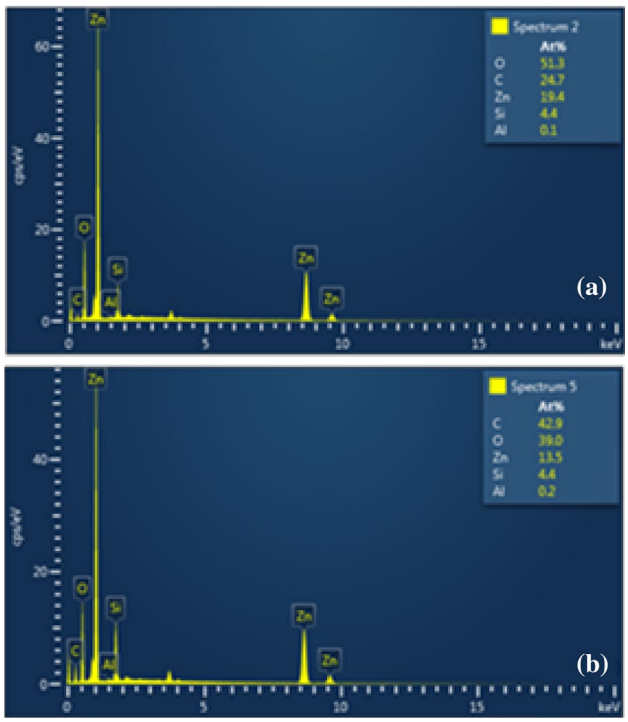

Fig. 3 EDX analysis of **a** rMWCNTs/ZnO and **b** eMWCNTs/ZnO nanocomposites

where, D is the grain size, k is a constant (0.94), λ is CuK_α radiation wavelength ($\lambda_{CuK\alpha} = 1.5418$ Å), β is FWHM and θ is Bragg angle. All the calculated parameters are given in Fig. 1b.

EDX measurements were carried out to evaluate the chemical composition of nanocomposites, given in Fig. 3. According to EDX analysis, the presence Zn, O and C elements were detected. Emerging silisium and aluminum elemental ratios were associated to amorphous glass substrate and experimental conditions. Etching of MWCNTs with aggressive acid were caused a decrease oxygen elemental ratio, indicating functional groups created by defect sites likely located at MWCNT surface [26]. Compared to ZnO seed layer samples in Ref. [19], rMWCNTs/ZnO and eMWCNTs/ZnO nanocomposites had lower oxygen elemental ratio due to the increasing adhesion between the layers with C coating on the ZnO seed layers.

It is well acknowledged that the working temperature is closely related to safety and energy consumption of a sensor, and the gas sensing performance of a chemiresistive semiconductor sensor is greatly influenced by operating temperature, as the temperature significantly affects the reaction kinetics and the gas adsorption and desorption processes on the surface of sensing materials [27, 28]. Figure 4a shows the transient response toward 50 ppm of CO with respect to the temperature from 30 to 180 °C. Studied sensors show a well-known sensor behavior which has maxima

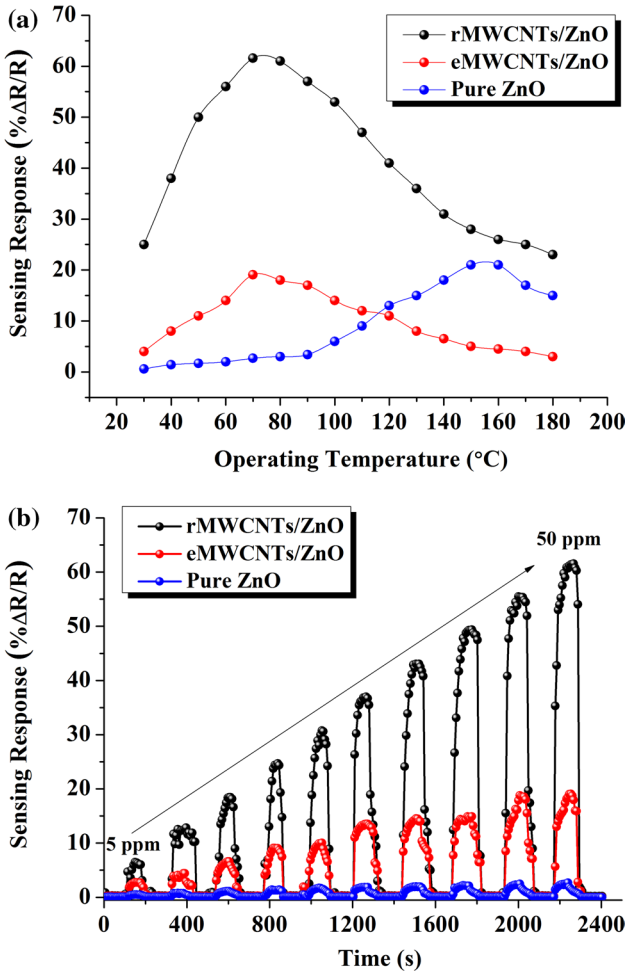

Fig. 4 The response of all sensors as a function of operating temperature (**a**) the dynamic gas sensing measurements (**b**)

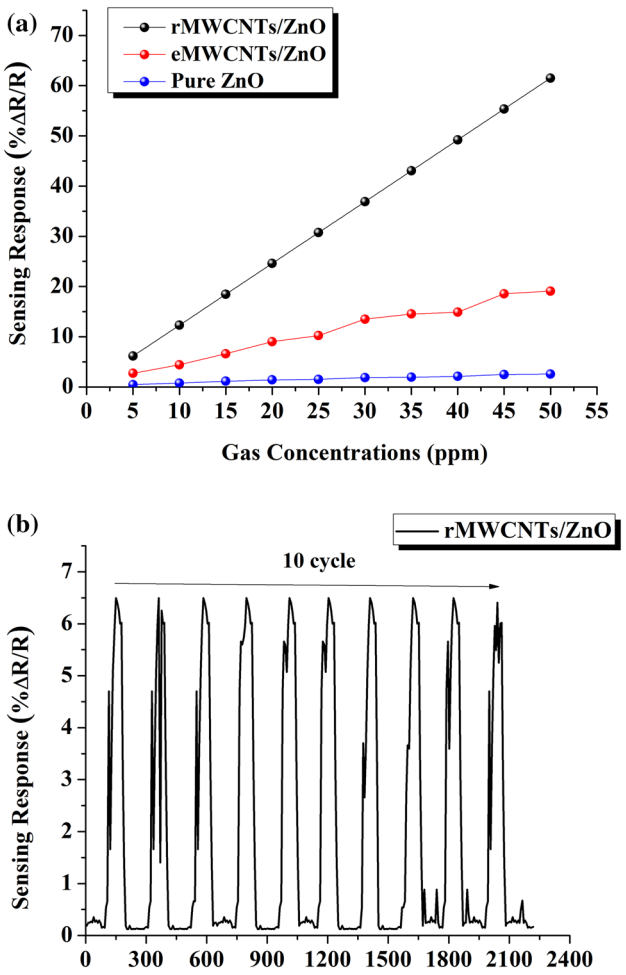

Fig. 5 The response versus gas concentrations of all sensors (**a**) the reproducibility of rMWCNTs/ZnO (**b**)

as a function of temperature. The response increases with increasing operating temperature, reaching a maximum sensitivity. The response decreased thereafter with a further increase in the operating temperature. The operating temperature was found 150 °C for pure ZnO film. It is important to note that the decoration of MWCNT reduces the operating temperature to 70 °C along with enhancement in sensor response. The rMWCNTs/ZnO sensor is giving the highest sensing response of 62% at much lower operating temperature (70 °C) as compared to eMWCNTs/ZnO and pure ZnO sensor which gave a sensing response of 19% and 21% at an operating temperature of 70 °C and 150 °C respectively. This enhancement may be due to high conductivity of MWCNTs network which provides low resistance nanochannels for electrons to transfer through the ZnO lattice [29]. Also MWCNTs have high adsorption capacity due to the higher surface area which enhances the adsorption ability of the ZnO surface when decorated with MWCNTs and may be attributed to the diffusion of the target gas through MWCNTs nanochannels as well as the desorption of chemisorbed oxygen species.

Figure 4b depicts the dynamic gas sensing measurements of sensors. The reversible cycles of the response curves indicate that the responses of the gas sensors are stable and repeatable. Upon exposure to reducing gases, the sensor resistance decreased initially due to the release of free electrons, and then became saturated. In the process, stopping the gas supply, it was noticed that the resistance increased and nearly returned to its baseline value. Figure 5a shows the response transients versus gas concentrations. The responses increase with increasing gas concentrations. rMWCNTs/ZnO shows the better responses to CO gas especially in every concentration compared to other sensors. This is related to the MWCNTs agglomeration, which declines the effective contact between ZnO and MWCNTs-COOH. As reported in the literature, the etching process can be surface degradation and loss of properties of MWCNTs [30–32]. Compared to eMWCNTs/ZnO, rMWCNTs/ZnO sensor has a

more porous and intended structure of layers provides paths for gas molecules in order to properly diffuse [33].

rMWCNTs/ZnO sensor showed the best gas detection properties compared to other sensors, therefore, other gas detection parameters were only obtained for this sensor. The response and recovery time are important parameters to assess the suitability of sensing material as a useful sensor design [34]. The response time was calculated 2 s and recovery time was 3 s for 50 ppm CO gas. Figure 5b depicts the reproducibility of rMWCNTs/ZnO exposure to 10 cycle of CO gas at 70 °C. The reversible cycles of the response curves indicate that the responses of the gas sensors are stable and repeatable. Gas sensors intended for practical applications are required not only to have good response and repeatability but also to have quick response/recovery times to target gases. The obtained results demonstrate that the response/recovery times of proposed sensor are highly satisfactory as presented in Table 1. Comparison of performance of developed sensors in the determination of CO gas is listed in Table 1.

The gas-sensing mechanism of the metal oxide gas sensors such as ZnO can be explained by the surface depletion model reported in previous literatures [38]. It mainly depends on the change of the conductivity caused by the adsorption and desorption process of gas molecules on the surface of sensing materials. When the sensor is exposed to air atmosphere, the oxygen molecules can be adsorbed on the surface and capture free electrons from the conduction band [38]. Then the adsorbed oxygen will form the chemisorbed oxygen species O, which turns to an electron depletion layer on the surface and forms the potential barrier. When reducing gases such as CO react with the adsorbed oxygen, CO_2 is produced with a consequent release of electrons back to the conduction and increase in conductivity of the semiconductor [39].

It can be also deduced that ZnO surface have a major role on the sensing activity; meanwhile, the MWCNTs network can act as a scaffold for the formation of ZnO nanoparticles and may assist the electrical charge transfer of the system [40]. Although the sensing reaction takes place on ZnO grains, the interface between ZnO and the MWCNTs plays critical role in the sensing mechanism of MWCNTs/ZnO composites through influencing the electronic properties of ZnO. The reasons for the increasing sensitivity are the low resistance nanochannels, high surface area, and larger depletion region of MWCNTs/ZnO composite sensors. Because MWCNTs have a large surface to volume ratio, the surface area of the film is increased upon MWCNT incorporation. The larger specific surface area allows more gas molecules to be absorbed on the surface of the sensing film. By incorporation ofMWCNTs into ZnO film, the depletion region is expanded than pure ZnO film. The reason of expanded depletion region is the electrons move easily through π-bonding on surface of MWCNTs. From these reasons, oxidation and reduction occurring on the specific surface are increased, making the movement of the surface electrons quite rapid. The sensor resistance changes due to the increase in electron concentration resulting from oxidation and reduction reaction facilitated by the reaction gas, The reasons for this phenomen on are high electrical conductivity and increased surface area by MWCNT incorporation [29].

4 Conclusions

Flower-like patterned ZnO thin films were synthesized by using the spin coating method and decorated with MWCNTs. MWCNT walls with and without the etching using HCl was applied to the thin films. The gas-sensing results had been shown that the response had been dramatically enhanced with the decoration of MWCNTs and rMWCNTs/ZnO sensor had exhibited the highest response to CO gas at 70 °C. Consequently, it had been determined that gas sensing performance of the MWCNTs-decorated ZnO sensors had improved surface reactions with ZnO lattice. This may be attributed to the diffusion of the target gas through MWCNTs nanochannels. It was observed that MWCNTs-incorporated ZnO sensors had low sensor resistance, high surface area, and larger depletion region. This study not only sheds light into the fundamental understanding of the gas

Table 1 Comparison of different developed sensors used in determination of CO gas

Material	Temperature (°C)	CO gas concentration (ppm)	Sensing response (%)	Response time (s)	Recovery time (s)	Reference
ZnO/MWCNT	70	50	13	5.8	12.1	Ref [11]
ZnO/MWCNT	RT	40	24	8	–	Ref [9]
ZnO/MWCNT	400	50	7	–	–	Ref [10]
SnO_2/MWCNT	150	100	8.8	52	10.2	Ref [35]
CO/MWCNT	RT	200	0.19 mV/ppm	23	35	Ref [36]
Au-MWCNT-SnO_2	250	50	74.6	–	–	Ref [37]
ZnO/MWCNT	70	25	62	2	3	This work

sensing for metal oxide semiconductor thin film with decoration of MWCNTs, but also provides a promising approach to achieve efficient detection of CO gas at low operating temperature.

References

1. R. Dhahri, M. Hjiri, L.El Mir, A. Bonavita, D. Iannazzo, M. Latino, N. Donato, S.G. Leonardi, G. Neri, J. Phys. D (2016) https://doi.org/10.1088/0022-3727/49/13/135502
2. Y. Aubard, N. Nadores, M.Cantaloube, Br. J. Obstet. Gynaecol. (2000) https://doi.org/10.1016/S0301-2115(00)00282-7
3. Q. Zhou, W. Chen, L. Xu, R. Kumar, Y. Gui, Z. Zhao, C. Tang, S. Zhu, Ceram. Int. (2018) https://doi.org/10.1016/j.ceramint.2017.12.038
4. M. Subası, B. Karsli, P. Yarbil, S. Zengin, Am. J. Emerg. Med. (2012) https://doi.org/10.1016/j.ajem.2012.03.011
5. X.J. Wang, W. Wang, Y.-L. Liu, Sens. Actuators B (2012) https://doi.org/10.1016/j.snb.2012.04.084
6. A. Nebatti, C. Pflitsch, B. Atakan, Thin Solid Films (2017) https://doi.org/10.1016/j.tsf.2017.07.002
7. S.K. Swain, I. Jena, Asian J. Chem. (2010) https://doi.org/10.5772/18423
8. Y. Liu, Polym. J. (2016) https://doi.org/10.1038/pj.2015.132
9. N.D. Alharbi, M.S. Ansari, N. Salah, S. Khayyat, Z.H. Khan, J. Nanosci. Nanotechnol. (2016) https://doi.org/10.1166/jnn.2016.10629
10. R.C. J.Khanderi, A.Gurlo Hoffmann, J.J. Schneider, J. Mater. Chem. (2009) https://doi.org/10.1039/b904822g
11. M. T.Hojati.R.Afzalzadeh Ebrahimi, Mater. Chem. Phys. (2018) https://doi.org/10.1016/j.matchemphys.2017.12.043
12. N.L.W. Septiani, B.Y. Nugraha, H.K. Dipojono, Appl. Phys. A. (2017) https://doi.org/10.1007/s00339-017-0803-y
13. A. Ayeshamariam, D. Saravanakkumar, M. Kashif, S. Sivaranjani, B. Ravikuma, Mech. Adv. Mater. Mod. Process. (2016) https://doi.org/10.1186/s40759-016-0010-0
14. E.C. Dandley, A.J. Taylor, K.S. Duke, M.D. Ihrie, K.A. Shipkowski, G.N. Parsons, J.C. Bonner, Part Fibre Toxicol. (2016) https://doi.org/10.1186/s12989-016-0141-9
15. M.T. Humayun, R. Divan, L. Stan, A. Gupta, D. Rosenmann, L. Gundel, P.A. Solomon, I. Paprotny, J. Vac. Sci. Technol. B (2015) https://doi.org/10.1116/1.4931694
16. P. Potirak, W. Pecharapa, W. Techitdheera, J. Exp. Nanosci. (2014) https://doi.org/10.1080/17458080.2013.820848
17. A. Ramar, T. Soundappan, S. Chen1, M. Rajkumar, S. Ramiah, Int. J. Electrochem. Sci., 7, (2012)
18. R. Vyas, S. Sharma, P. Gupta, A.K. Prasad, A.K. Tyagi, K. Sachdev, S.K. Sharma, Adv. Mater. Res. (2012) https://doi.org/10.4028/www.scientific.net/AMR.585.235
19. F. Özütok, S. Demiri, Digest J. Nanomater. Biostruct. **12**, 309–315 (2017)
20. I. Karaduman, E. Er, H. Celikkan, S. Acar, Sens. Actuators B (2015) https://doi.org/10.1016/j.snb.2015.07.063
21. I. Karaduman, M. Demir, D.E. Yıldız, S. Acar, Phys. Scr. **90**, 055802 (2015)
22. S.H. Largani, M.A. Pasha, Int. Nano Lett. (2017) https://doi.org/10.1007/s40089-016-0197-4
23. N.K. Allouche, T.B. Nasr, N.T. Kamouna, C. Guasch, Mater. Chem. Phys. (2010) https://doi.org/10.1016/j.matchemphys.2010.05.026
24. M. Lu, W. Cao, H. Shi, X. Fang, J. Yang, Z. Hou, H. Jin, W. Wang, J. Yuan, M.S. Cao, J. Mater. Chem. A (2014) https://doi.org/10.1039/c4ta01715c
25. F. Avilés, J.V. Cauich-Rodríguez, J.A. Rodríguez-González, A. May-Pat, Express Polym. Lett. **5**(9), 766–776 (2011)
26. R. Das, M.E. Ali, S.B.A. Hamid, M.S.M. Annuar, S. Ramakrishna, J. Nanomater. (2014) https://doi.org/10.1155/2014/945172
27. B.-Y. Wang, D.-S. Lim, Y.-J. Oh, Jpn. J. Appl. Phys. **52**, 101103 (2013)
28. M. Narjinary, P. Rana, A. Sen, M. Pal, Mater. Des. **115**, 158–164 (2017)
29. H. Kim, M. Hong, H.W. Jang, S. Yoon, H. Park, Thin Solid Films (2013) https://doi.org/10.1016/j.tsf.2012.07.062
30. S. Maity, N. Sankar Das, K. Kumar, Chattopadhyay, Phys. Status Solidi B **250**(9), 1919–1925 (2013)
31. E.T. Mombeshora, P.G. Ndungu, A.L. Leigh Jarvis, V.O. Nyamori, Int. J. Energy Res. **41**, 1182–1201 (2017)
32. Q.-Q. Fan, Z.-Y. Qin, X. Liang, L. Li, W.-H. Wu, M.-F. Zhua, J. Exp. Nanosci. **5**(4), 337–347 (2010)
33. K. Müller, E. Bugnicourt, M. Latorre, M. Jorda, Y.E. Sanz, J.M. Lagaron, O. Miesbauer, A. Bianchin, S. Hankin, U. Bölz, G. Pérez, M. Jesdinszki, M. Lindner, Z. Scheuerer, S. Castelló, M. Schmid, Nanomaterials (2017) https://doi.org/10.3390/nano7040074
34. S. Galioglu, I. Karaduman, T. Çorlu, B. Akata, M.A. Yıldırım, A. Ateş, S. Acar, J. Mater. Sci. **29**(2), 1356–1368 (2018)
35. S.B. Naghadeh, S. Vahdatifar, Y. Mortazavi, A.A. Khodadadi, A.Abbasi, Sen. Actuators B (2015) https://doi.org/10.1016/j.snb.2015.09.088
36. Y. C.Dai.C. Chen.C.Kuo Wu, Sensors (2010) https://doi.org/10.3390/s100301753
37. R. Ionescu, E.H. Espinosa, R. Leghrib, A. Felten, J.J. Pireaux, R. Erni, G. Van Tendeloo, C.Bittencourt, N. Canellas, E. Llobet, Sensors and Actuators B (2008) https://doi.org/10.1016/j.snb.2007.11.001
38. D. Han, L. Zhai, F. Gu, Z. Wang, Sens. Actuators B **262**, 655–663 (2018)
39. S. Benkara, S. Zerkout, H. Ghamrid, Mater. Sci. Semicond. Process. **16**(5), 1271–1279 (2013)
40. G. Karim-Nezhad, A. Sarkary, Z. Khorablou, P.S. Dorraji, Iran. J. Pharm. Res. **17**(1), 52–62 (2018)